Biogeosciences Discuss., 9, 5887–5927, 2012
www.biogeosciences-discuss.net/9/5887/2012/
doi:10.5194/bgd-9-5887-2012

Biogeosciences
Discussions

Methane emissions associated with the conversion of marshland to cropland and climate change on the Sanjiang Plain of Northeast China from 1950 to 2100

T. Li[1], Y. Huang[2], W. Zhang[1], and Y. Q. Yu[1]

[1]State Key Laboratory of Atmospheric Boundary Layer Physics and Atmospheric Chemistry, Institute of Atmospheric Physics, Chinese Academy of Sciences, Beijing 100029, China
[2]The State Key Laboratory of Vegetation and Environmental Change, Institute of Botany, Chinese Academy of Sciences, Beijing 100093, China

Received: 17 March 2012 – Accepted: 27 April 2012 – Published: 24 May 2012

Correspondence to: W. Zhang (zhw@mail.iap.ac.cn)

Published by Copernicus Publications on behalf of the European Geosciences Union.

Abstract

Wetland loss and climate change are known to alter regional and global methane (CH_4) budgets. Over the last six decades, an extensive area of marshland has been converted to cropland on the Sanjiang Plain in Northeast China, and a significant increase in air temperature has also been observed there, while the impacts on regional CH_4 budgets remain uncertain. Through model simulation, we estimated the changes in CH_4 emissions associated with the conversion of marshland to cropland and climate change in this area. Model simulations indicated a significant reduction of 1.1 $\mathrm{Tg\,yr^{-1}}$ from the 1950s to the 2000s in regional CH_4 emissions. The cumulative reduction of CH_4 from 1960 to 2009 was estimated to be ~ 36 Tg relative to the 1950s, and marshland conversion and the climate contributed 86 % and 14 % of this change, respectively. Interannual variation in precipitation (linear trend with $P > 0.2$) contributed to yearly fluctuations in CH_4 emissions, but the relatively lower amount of precipitation over the period 1960–2009 (47 $\mathrm{mm\,yr^{-1}}$ lower on average than in the 1950s) contributed ~ 91 % of the reduction in the area-weighted CH_4 flux. Global warming at a rate of 0.3 °C per decade ($P < 0.001$) has increased CH_4 emissions significantly since the 1990s. Relative to the mean of the 1950s, the warming-induced increase in the CH_4 flux has averaged 19 $\mathrm{kg\,ha^{-1}\,yr^{-1}}$ over the last two decades. For the RCP 2.6, RCP 4.5, RCP 6.0 and RCP 8.5 scenarios of the fifth IPCC assessment report (AR5), the CH_4 flux is predicted to increase by 36 %, 52 %, 78 % and 95 %, respectively, by the 2080s compared to 1961–1990 in response to climate warming and wetting.

1 Introduction

Methane (CH_4) is recognized as one of the most potent greenhouse gases; it is 25 times more powerful than carbon dioxide (CO_2) in terms of its global warming potential (IPCC, 2007). Although natural wetlands cover only 5–8 % of the earth's land surface area (Ramsar Convention Secretariat, 2004; Mitsch and Gosselink, 2007), they contribute 20–25 % of the total annual CH_4 emissions (IPCC, 2007; Mitsch and Gosselink, 2007).

The regional and global CH_4 budgets of wetlands are influenced by large-scale processes, such as the conversion of wetlands to other uses (Bridgham et al., 2006; Huang et al., 2010) and climate change (Cao et al., 1998; Gedney et al., 2004; Shindell et al., 2004). Half of the world's wetlands were lost during the 20th century (Revenga et al., 2000). In China, approximately 20 % of the wetlands were lost from 1950 to 2000, and 82 % of the loss has been attributed to agricultural use (An et al., 2007). Climate change, particularly in terms of temperature (Charmann and Hendon, 2000) and precipitation (Cao et al., 1998; Charmann and Hendon, 2000; Vepraskas and Caldwell, 2008), alters the biochemical processes involved in CH_4 production, oxidation and emission (Strack et al., 2008; Updegraff et al., 2001).

The Sanjiang Plain, located in Northeast China, was formerly the largest marshland complex in China (Huang et al., 2010; Wang et al., 2006). In the 1950s, the wetland area of the Sanjiang Plain (Liu and Ma, 2000) accounted for ~ 70 % of Heilongjiang province and ~ 40 % of Northeast China (Ning et al., 2008). However, an extensive area of marshland has been converted to cropland over the last six decades in this region (Liu and Ma, 2000; Zhang et al., 2003; Huang et al., 2010). Meanwhile, a significant increase in the surface air temperature has been detected (Ding and Cai, 2007), occurring at a rate of 0.3 °C per decade, and annual precipitation declined at a rate of 15 mm per decade from 1950 to 2000 in Northeast China (Zhao et al., 2009). Furthermore, significant warming has been predicted to occur under different scenarios by the end of the 21st century (SRES A2, B2 for IPCC AR4 and RCPs for IPCC AR5) (Editorial Committee of China's National Assessment Report on Climate Change, 2007; Bernie, 2010). By 2100, the temperature is projected to increase by 4.5 °C or 6.1 °C, while precipitation will increase by 12 % or 13 % in Northeast China under the SRES B2 and A2 scenarios, respectively (Editorial Committee of China's National Assessment Report on Climate Change, 2007).

Researchers have attempted to understand the effects of temperature and precipitation on seasonal variation in CH_4 fluxes in site-specific studies (Yang et al., 2006; Song et al., 2009) to estimate regional CH_4 emissions by extrapolating field measurements to the region (Cui, 1997; Ding et al., 2004; Ding and Cai, 2007) and to quantify regional CH_4 emissions associated with marshland conversion on the Sanjiang Plain (Huang et al., 2010), whereas less attention has been given to an integrated evaluation of CH_4 emissions in relation to marshland conversion and climate change.

Recognizing the significance of wetlands in regional CH_4 budgets, this study focuses on quantifying the variation in CH_4 emissions on the Sanjiang Plain of Northeast China via model simulations. The objectives of this study are to estimate the change in regional CH_4 emissions associated with the conversion of marshland to cropland and climate change and to identify the contributions of the conversion of marshland to cropland and climatic factors to the changes in CH_4 emissions over the period of 1950–2009. We also make predictions regarding the impact of climate change on the CH_4 flux from the marshland extending to the year 2100.

2 Materials and methods

2.1 Research area

The research area lies on the Sanjiang Plain, situated in the eastern part of Heilongjiang Province, Northeast China (Fig. 1). It is located between 43°50′ N and 48°28′ N latitudinally and between 129°11′ E and 135°05′ E longitudinally, with a total area of 11.89 million ha (Zhang et al., 2006) covering 23 counties and 3 administrative farms (see Supplement A for more details).

The study area is characterized by a temperate humid and subhumid continental monsoon climate with an annual mean temperature of ~ 2.5 °C. Annual rainfall ranges from 350 to 770 mm, with 80 % occurring from May to September. The freshwater marsh is mainly dominated by *Carex* plants and *Deyeuxia angustifolia*, which generally begin growing in late May and senesce in late September. The above-ground biomass ranges from 500 to 700 $\mathrm{g\,m^{-2}}$ (Hao, 2006; Yang et al., 2002; Zhang et al., 2007).

After marshland conversion, the cropland became the dominant landscape on the Sanjiang Plain (Zhang et al., 2010). By now, the main species of crops on the Sanjiang Plain are soybean, corn and rice (Heilongjiang Provencal Bureau of Statistics, 2010). Irrigated rice harvests once per year. The rice growing season is generally from May to September. The average grain yield of rice over the period of 2000–2009 was 6.4 $\mathrm{t\,ha^{-1}}$ (Heilongjiang Provencal Bureau of Statistics, 2010).

2.2 The modeling approach

Two biogeophysical models, CH4MOD and CH4MOD$_{\text{wetland}}$, were used to simulate CH_4 emissions from an area of irrigated rice cultivation and a natural marshland, respectively. Both of the models have great potential for scaling up because they have provided realistic estimates of observed results from various types of rice paddies and natural wetlands, respectively. To quantify the individual factorial impact on CH_4 emissions from marshland, we performed several simulation experiments using CH4MOD$_{\text{wetland}}$.

2.2.1 CH4MOD for irrigated rice cultivation

CH4MOD was developed to predict methane emissions from rice paddy soils. The model associated this process with rice growth, organic C depletion and environmental factors (Huang et al., 2004). The model's input parameters included the rice grain yield, the soil sand percentage, the amount of organic amendment, the initial fractions of structural and non-structural carbohydrates in the incorporated organic matter, the water management pattern, and the daily air temperature. The outputs are the daily and annual rates of CH_4 production and emissions. The model was validated against a total of 94 field observations that covered the main rice cultivation regions from Northern (Beijing, 40°30′ N, 116°25′ E) to Southern (Guangzhou, 23°08′ N, 113°20′ E) China and from Eastern (Hangzhou, 30°19′ N, 120°12′ E) to Southwestern (Tuzu, 29°40′ N, 103°50′ E) China. This model can reasonably simulate CH_4 emission from irrigated rice fields (Huang et al., 2004).

2.2.2 CH4MOD$_{\mathrm{wetland}}$ for natural wetlands

CH4MOD$_{\mathrm{wetland}}$ was developed based on CH4MOD to predict CH_4 emissions from natural wetlands (Li et al., 2010). The model adopted the rationale of CH4MOD and focused on the supply of methanogenic substrates in natural wetlands that differs from the supply in rice paddies. The input variables include environmental variables, soil properties and plant growth-related controls. The outputs are the daily and annual rates of CH_4 production and emissions. CH4MOD$_{\mathrm{wetland}}$ was validated against independent field measurements of CH_4 emissions from different wetland sites, including a marshland on the Sanjiang Plain (Northeast China), a peatland on the Ruoergan Plateau (Southwest China), a fen in Saskatchewan (Canada) and bogs in Michigan (USA). Model validation showed that CH4MOD$_{\mathrm{wetland}}$ was generally capable of simulating the seasonal and interannual variations in CH_4 emissions from different sites, especially in Northeast China (Li et al., 2010).

A previous study employed observed daily standing water depth data to drive CH4MOD$_{\mathrm{wetland}}$ (Li et al., 2010). When applying this model on a regional scale, these input data should be simulated. To obtain water table dynamics, empirical equations were used because they require fewer inputs and are suitable for small-scale studies such as that of Northeast China (Li et al., 2004). Water table dynamics (WT, in cm) are determined directly by the balance between the water input (S_{in}, cm), runoff (F_{out}, cm) and evapotranspiration (ET, cm). No runoff occurs during the period of freezing temperatures from November to March:

$$\Delta WT = \begin{cases} S_{\mathrm{in}} - F_{\mathrm{out}} - ET & \text{(Apr–Oct)} \\ P - ET & \text{(Nov–Mar)} \end{cases}, \tag{1}$$

$$WT_i = WT_{i-1} + \Delta WT, \tag{2}$$

where WT_i represents the daily water table. Using Wetland-DNDC, S_{in} is a function of precipitation (P), and F_{out} includes surface outflow and ground outflow, both of which are determined by the water table (Zhang et al., 2002). The Priestley-Taylor model (Priestley and Tayler, 1972; Shuttleworth, 1992) was used to calculate ET (Sun and Song, 2008). The net radiation (R_{n}), which is used to calculate ET in the Priestley-Taylor model, was calculated using the equations of the modified Penmann-Monteith model (Allen et al., 1998). When the water table position value was less than zero, the standing water depth (WD) in CH4MOD$_{\mathrm{wetland}}$ was considered to be zero.

The experimental constants (α_0, a_1, a_2, D_1, D_2) in the functions calculating S_{in} and F_{out} from Wetland-DNDC were calibrated by trial and error (Zhang et al., 2002). The values of the experimental constants for the main types of marshland on the Sanjiang Plain are shown in Supplement B (Table B1).

2.2.3 Simulation climatic factor impacts

The climatic factors considered in CH4MOD$_{\mathrm{wetland}}$ and the empirical water table model include air temperature (T_{air}), precipitation (P) and net radiation (R_{n}). To quantify the impacts of climatic factors on the change in regional CH_4 emissions and area-weighted CH_4 fluxes from marshland on the Sanjiang Plain, many simulations were conducted under both real climate conditions and different climate scenarios (Table 1) using CH4MOD$_{\mathrm{wetland}}$. Table 1 provides a description of the real climate condition and four climate scenarios. The real climate condition ($A_{T,P,R\mathrm{n}}$) means that observed data were used for all of the climatic factors (Table 1). $S_{T,P,R\mathrm{n}}$ assumed that the annual mean T_{air}, P and R_{n} of the last five decades were the same as in the 1950s, as if there was no climate change during the last six decades (Table 1). $S_{T,P}$ assumed that T_{air} and P from 1960 to 2009 were the same as in the 1950s, while observed data were used for R_{n} (Table 1). Similarly, S_T and S_P assumed that only T_{air} or P was the same as in the 1950s, respectively (Table 1).

$S_{T,P}$ (Table 1) is used as an example to explain how we simulated the annual CH_4 flux for each county or administrative farm and annual regional CH_4 emissions from the marshland of the Sanjiang Plain under the specified scenario. First, we randomly selected one year from 1950 to 1959 a total of 50 times and used the daily air temperature and the daily precipitation data series for the selected years to replace the corresponding climate data series of 1960, 1961 ... 2009. The new T_{air} and P data series and the observed daily R_{n} data series for 1950–2009 were used to drive the model to simulate the annual $\mathrm{CH_4}$ flux for each county or administrative farm. Then, the above program was repeated 10 times to reduce the uncertainty caused by random selection. The average result of the 10 simulations is the annual $\mathrm{CH_4}$ flux under $S_{T,P}$ for the kth county or administrative farm in the ith year $F^{i,k}_{S_{T,P}}$ ($\mathrm{kg\,ha^{-1}\,yr^{-1}}$). $T^{i}_{S_{T,P}}$ ($\mathrm{Tg\,yr^{-1}}$) represents the regional $\mathrm{CH_4}$ emissions in the ith year under $S_{T,P}$, which is calculated using the following equation:

$$T^{i}_{S_{T,P}} = \sum_{k=1}^{23} F^{i,k}_{S_{T,P}} \times \left(A^{i-1,k} - \mathrm{AC}^{i-1,k}\right)/10^{9} \tag{3}$$

where $A^{i-1,k}$ (ha) represents the marshland area of the kth county or administrative farm in the $(i-1)$th year, and $\mathrm{AC}^{i-1,k}$ (ha) represents the yearly area of marshland converted to cropland of the kth county or administrative farm in the $(i-1)$th year.

Similarly, the annual regional $\mathrm{CH_4}$ emissions under scenario $S_{T,P,R\mathrm{n}}$ ($T^{i}_{S_{T,P,R\mathrm{n}}}$ in $\mathrm{Tg\,yr^{-1}}$), S_T ($T^{i}_{S_T}$ in $\mathrm{Tg\,yr^{-1}}$) and S_P ($T^{i}_{S_P}$ in $\mathrm{Tg\,yr^{-1}}$) (Table 1) can be calculated in the same way as scenario $S_{T,P}$.

The difference in simulated $\mathrm{CH_4}$ emissions (including the area-weighted $\mathrm{CH_4}$ flux and regional $\mathrm{CH_4}$ emissions) under $A_{T,P,R\mathrm{n}}$ compared to the appointed climate scenario (Table 1) could represent the impact of the corresponding climatic factors on $\mathrm{CH_4}$ emissions (Eqs. 4 and 5). The difference in the simulated $\mathrm{CH_4}$ emissions under $A_{T,P,R\mathrm{n}}$ compared to $S_{T,P,R\mathrm{n}}$ is considered to be the impact of T_{air}, P and R_{n} on $\mathrm{CH_4}$ emissions. Similarly, the difference in simulated $\mathrm{CH_4}$ emissions under $A_{T,P,R\mathrm{n}}$ compared to $S_{T,P}$ is considered to be the impact of T_{air} and P on $\mathrm{CH_4}$ emissions. The differences in simulated CH_4 emissions under $A_{T,P,Rn}$ compared to S_T and S_P are considered to be the impacts of T_{air} and P on CH_4 emissions, respectively.

When analyzing the impact of climatic factors on regional CH_4 emissions, the concomitant impact of marshland conversion could not be isolated. The impact of the specified climatic factors on the change of the regional CH_4 emissions in the jth decade ($\mathrm{IT}^j_{\mathrm{CF}}$ in Tg per decade) was calculated by:

$$\mathrm{IT}^j_{\mathrm{CF}} = \sum_i (T^i_{A_{T,P,Rn}} - T^i_{S_{\mathrm{CF}}}), \tag{4}$$

where $T^i_{A_{T,P,Rn}}$(Tg yr^{-1}) and $T^i_{S_{\mathrm{CF}}}$ (Tg yr^{-1}) represent the annual regional CH_4 emissions under $A_{T,P,Rn}$ and the appointed climate scenario (indicated by the subscript S_{CF}) in the ith year, respectively. The subscript CF in $\mathrm{IT}^j_{\mathrm{CF}}$ (Tg per decade) and S_{CF}represents the specified climatic factors. For example, when CF represents T_{air}, P and R_{n}, $\mathrm{IT}^j_{T,P,Rn}$ (Tg per decade) represents the impact of T_{air}, P and R_{n} on regional CH_4 emissions, and $T^i_{S_{T,P,Rn}}$ (Tg yr^{-1}) represents the annual regional CH_4 emissions under scenario $S_{T,P,Rn}$.

When analyzing the independent impacts of climatic factors on the area-weighted CH_4 flux, we sought to isolate the impact of marshland conversion. Assuming that no marshland was converted to cropland during the last 60 yr, the area-weighted CH_4 flux (F^i in kg ha^{-1} yr^{-1}), derived from the proportion of the original area in each county or administrative farm within the total area of Sanjiang Plain in 1950, was used to calculate the independent impact of the climatic factors on the CH_4 flux as follows:

$$\mathrm{IF}^i_{\mathrm{CF}} = F^i_{A_{T,P,Rn}} - F^i_{S_{\mathrm{CF}}}, \tag{5}$$

$$P^j_{\mathrm{CF}} = \frac{\overline{\mathrm{IF}^j_{\mathrm{CF}}}}{F^{1950s}_{A_{T,P,Rn}}}, \tag{6}$$

where $\mathrm{IF}^i_{\mathrm{CF}}$ (kg ha^{-1} yr^{-1}) represents the impact of the specified climatic factors (indicated by the subscript CF) on the change in the area-weighted CH$_4$ flux in the ith year, and $F^i_{A_{T,P,Rn}}$ (kg ha^{-1} yr^{-1}) and $F^i_{S_{\mathrm{CF}}}$ (kg ha^{-1} yr^{-1}) represent the area-weighted CH$_4$ flux under $A_{T,P,Rn}$ and the climate scenario (indicated by the subscript S_{CF}) in the ith year, respectively. $\overline{\mathrm{IF}^j_{\mathrm{CF}}}$ (kg ha^{-1} yr^{-1}) represents the average impact of climatic factors on the area-weighted CH$_4$ flux in the jth decade. $\overline{F^{1950s}_{A_{T,P,Rn}}}$ (kg ha^{-1} yr^{-1}) represents the average area-weighted CH$_4$ flux under $A_{T,P,Rn}$ in the 1950s assuming that no marshland conversion occurred. P^j_{CF} represents the proportion of $\overline{\mathrm{IF}^j_{\mathrm{CF}}}$ to the average area-weighted CH$_4$ flux under $A_{T,P,Rn}$ in the 1950s in the jth decade. The subscript CF in $\mathrm{IF}^i_{\mathrm{CF}}$, S_{CF}, P^j_{CF} and $\overline{\mathrm{IF}^j_{\mathrm{CF}}}$ is the same as in Eq. (3).

2.2.4 Predictions of the impact of climate change on CH$_4$ fluxes

The climate change scenarios used in this study were RCP 2.6, RCP 4.5, RCP 6.0 and RCP 8.5, which were projected by the Flexible Global Ocean-Atmosphere-Land System climate model (FGOALS, Yu et al., 2002, 2004). More information about the RCP scenarios is given in Supplement C.

FGOALS is a GCM (General Circulation Model) that contributed to the 5th assessment report (AR5) of the IPCC. It has a spatial resolution of 1.65° latitude by 2.8° longitude. The outputs of FGOALS were spatially downscaled to the 7 meteorological stations across the Sanjiang Plain using the delta change method (Hay et al., 2000; Beldring et al., 2008; Prudhomme et al., 2002). The delta change method is used to compute differences between current and future GCM simulations and to add these changes to observed time series (Hay et al., 2000). In this study, we chose the representative long-term average of 1961–1990 as the current or baseline period (Prudhomme et al., 2002; Wilby et al., 2004), as this is the standard World Meteorological Organization period (Hulme et al., 1995). The simulated average area-weighted CH$_4$

Title Page
Abstract | Introduction
Conclusions | References
Tables | Figures
◀I | ▶I
◀ | ▶
Back | Close
Full Screen / Esc
Printer-friendly Version
Interactive Discussion

flux for 1961–1990 represents the baseline CH_4 flux from the marshland of the Sanjiang Plain. We focused on the future time horizons of the 2030s (2011–2040), 2050s (2041–2070) and 2080s (2071–2100). CH_4 fluxes were simulated for each county or administrative farm using CH4MOD$_{\mathrm{wetland}}$, which was driven by the downscaled output data from FGOALS. The area-weighted CH_4 flux for 2010–2100 is derived from the proportion of the marshland area in each county or administrative farm within the whole area of the Sanjiang Plain in 2009. The changes in the average area-weighted CH_4 fluxes for the 2030s, 2050s and 2080s relative to the baseline CH_4 flux represent the predicted impact of climate change on CH_4 fluxes from the marshland of the Sanjiang Plain.

2.3 Data sources

2.3.1 Changes in area of marshland and rice paddies

It is reported that wetland loss in Northeast China is mainly caused by reclamation (Liu and Ma, 2000; Gong et al., 2010; An et al., 2007). According to Wang et al. (2009), an estimated 2.58 Mha of marshland was converted to cropland on the Sanjiang Plain over the period from 1954–2005, which is compared to an increase of the cropland area from the official statistical reports (Su and Zhang, 2008) from the 1950s to the 2000s. Therefore, we used the yearly increase in cropland area taken from the annual statistical reports for a county or at the scale of an administrative farm (Su and Zhang, 2008) to calculate the yearly area of marshland converted to cropland from 1950 to 2009. The marshland area in each county in 1950 was calculated by totaling the cropland area (Su and Zhang, 2008) and marshland area (Wang et al., 2002) in 1980 and then subtracting the cropland area from 1950 (Su and Zhang, 2008). The marshland area on administrative farms in 1950 was obtained from the local chronicles of the reclamation system of Heilongjiang province (http://www.zglz.gov.cn/nongken/index.html). According to Cui (1997), the marshland area is mainly vegetated with *Deyeuxia angustifolia* and *Carex* plants, which account for approximately 20 % and 80 % of the vegetation on the Sanjiang Plain, respectively.

The yearly acreage and yields of irrigated rice from 1950 to 2009 were obtained from the statistical yearbook of Heilongjiang province at the scale of a county or an administrative farm.

2.3.2 Model input data

The environmental drivers of CH4MOD$_{\text{wetland}}$ include the daily air temperature and standing water depth (Li et al., 2010). Meteorological datasets from 7 meteorological stations across the Sanjiang Plain from 1950–2009 were acquired from the China Meteorological Administration (CMA) (http://cdc.cma.gov.cn/). Daily standing water depth data were calculated using the empirical water table model. Inputs for the empirical water table model, such as daily precipitation, hours of sunshine, maximum/minimum temperatures, and relative humidity, were also obtained from the CMA. The projected meteorological datasets were outputs of FGOALS, which were provided by the State Key Laboratory of Numerical Modeling for Atmospheric Sciences and Geophysical Fluid Dynamics (LASG), Institute of Atmospheric Physics (IAP), Chinese Academy of Sciences (CAS). For counties or administrative farms for which meteorological data were not available, we used the data from the neighboring site. The plant and soil input parameters of CH4MOD$_{\text{wetland}}$ were described by Li et al. (2010).

Field measurements of the water table and the annual CH_4 flux in marshlands of *Deyeuxia angustifolia* from 2003 to 2004 and *Carex lasiocarpa* from 2003 to 2005 (Hao, 2006; Song et al., 2007) were used to calibrate and validate the empirical water table model. However, the above papers (Hao, 2006; Song et al., 2007) only report the CH_4 fluxes in the growing season. According to Yang et al. (2006), the CH_4 flux in the non-growing season (November to March) represents ~ 4 % of the total yearly flux on the Sanjiang Plain. This relationship was used to calculate the annual CH_4 flux in this study. More details about these measurements were described by Li et al. (2010). Measurements of the daily evapotranspiration and net radiation on the Sanjiang Plain during the period from 2005 to 2007 (Zhao et al., 2008; Jia et al., 2010) were used to validate the intermediate results of the empirical water table model.

For CH4MOD, the environmental driver is the daily air temperature. The database of input parameters was described by Huang et al. (2006).

3 Results and discussion

3.1 Model validation and sensitivity analysis

Figure 2 shows the seasonal patterns of the simulated and observed standing water depth and CH_4 emissions for a *Deyeuxia angustifolia* marsh site (Fig. 2a, c) and a *Carex lasiocarpa* marsh site (Fig. 2b, d) on the Sanjiang plain. The model can basically simulate the seasonal variations in standing water depth (Fig. 2a, b) and CH_4 fluxes (Fig. 2c, d). The empirical water table model underestimated the standing water depth from April to July 2003 and overestimated the standing water depth from September to October 2003 for the *Deyeuxia angustifolia* site (Fig. 2a). Correspondingly, a systematic negative discrepancy occurred during the period from April to July 2003, and a positive discrepancy occurred during the period from September to October 2003 between the modeled and observed CH_4 emissions from the *Deyeuxia angustifolia* site (Fig. 2c). For the *Carex lasiocarpa* site, the empirical water table model underestimated the standing water depth from April to July of 2004 and 2005 (Fig. 2b). However, the simulated CH_4 flux matches the observed flux well during the same period (Fig. 2d). This correspondence occurred because in $\mathrm{CH4MOD_{wetland}}$, CH_4 emissions are not sensitive to the standing water depth when it is aboveground for a period (Li et al., 2010), which is in agreement with the observation of Thomas et al. (2009) that the soil redox potential decreases to a certain limit and maintains that level when the standing water depth is above the soil surface for a given amount of time.

Figure 3 shows the observed and simulated CH_4 emissions from the Sanjiang Plain. Using 273 datasets, regression of the observed versus simulated CH_4 fluxes produced an R^2 of 0.49 with a slope of 0.87 ($P < 0.001$) (Fig. 3a). The performance of CH4MOD$_{\text{wetland}}$ was good for the total annual/seasonal CH_4 amounts (Fig. 3b). Regression of the computed and observed annual CH_4 amounts yielded an R^2 of 0.74 with a slope of 1.00 ($n = 7$, $P < 0.01$) (Fig. 3b).

A sensitivity analysis was performed to reveal the effects of the environmental drivers and model inputs on CH_4 emissions from the *Deyeuxia angustifolia* and *Carex lasiocarpa* sites from 2003–2004 (Table 2). The sensitivity of the model was tested for the environmental drivers air temperature (T_{air} in °C) and standing water depth (WD in cm); the plant input parameter of the maximum above-ground biomass ($W_{\max}$ in g m^{-2}); and the soil input parameters of the sand fraction (SAND), the soil bulk density (ρ in g cm^{-3}) and the concentration of soil organic matter (SOM in g kg^{-1}). The sensitivity of a given factor to the model's output was quantified as the ratio of the change in total seasonal CH_4 emissions ($\Delta CH_4 = CH_4 - CH_{4\_\text{baseline}}$) to the CH_4 emissions at baseline (CH_{4_baseline}).

The sensitivity analysis shows that the environmental drivers (T_{air} and WD) are the most sensitive contributors to the CH_4 flux (Table 2). The response of the CH_4 fluxes to the standing water depth was more sensitive in a seasonally flooded wetland (*Deyeuxia angustifolia* site) than in a continuously flooded wetland (*Carex lasiocarpa* site) (Table 2). Among the model input parameters, the plant input parameter ($W_{\max}$) was more sensitive to the model output than the soil input parameters (SAND, ρ and SOM) (Table 2).

3.2 Decadal and spatial CH_4 variation from 1950–2009

3.2.1 Changes in marshland area due to the conversion of marshland to cropland

The marshland area on the Sanjiang Plain decreased by 3.2 Mha due to intensive cultivation over the period from 1950–2009 (Fig. 4). Extensive conversion of marshland to cropland occurred in the 1950s and 1970s when cropland increased at a rate of 0.05–0.06 $\mathrm{Mha\,yr^{-1}}$, and marshland loss occurred at a rate of $\sim$ 0.06 $\mathrm{Mha\,yr^{-1}}$. From 1960 to 1966, cropland increased by 0.54 Mha, and the loss of marshland was serious. However, from 1966 to 1970, grievous natural disasters (Group of Chinese Wetland Resources Development and Environmental Protection, 1998) caused farmers to lose their enthusiasm of cultivation and to abandon large areas of cropland (Ma, 1999). We assumed that the abandoned cropland was reverted to marshland; thus, the marshland area increased during the period from 1966–1970. From 1980 to 1999, marshland decreased at a rate of 0.03 $\mathrm{Mha\,yr^{-1}}$. During the 2000s, cropland increased extensively (Fig. 4), and marshland decreased by $\sim$ 1.1 Mha (Fig. 4).

The proportion of the area of irrigated rice was relatively low when marshland was converted to cropland before the mid-1990s, though it increased substantially thereafter (Fig. 4). In the 2000s, the irrigated rice area accounted for 33 % of the total cultivated area (Heilongjiang Provencal Bureau of Statistics, 2010). Table D1 (Supplement D) shows the spatiotemporal changes in the marshland and irrigated rice areas on the Sanjiang Plain.

Marshland on the Sanjiang Plain was converted for different land uses over the period from 1949–2000, including for cropland, grassland, woodland and urbanization (Wang et al., 2003; Zhang et al., 2010), which were unavailable to quantify not only in the yearly sequence from 1950 to 2009 but also at the county scale (Fig. 1). This study only focuses on the conversion of marshland to cropland (Fig. 4). Based on data retrieved from remote sensing images from 1976, 1986, 1995, 2000 and 2005, an estimated 2.58 Mha of marshland was converted to cropland on the Sanjiang Plain over the period of 1954–2005 (Wang et al., 2009), which agrees with our estimate of 2.45 Mha (from 1950–2005).

3.2.2 Decadal variation of CH_4 emissions

Based on the models and the statistical area datasets, the mean annual area-weighted CH_4 flux and the variation in regional CH_4 emissions in the marshland and rice paddies of the Sanjiang Plain were estimated for the past 6 decades (Fig. 5b). The variation in the mean annual area-weighted CH_4 flux from the marshland was mainly influenced by the climate. The minimum area-weighted CH_4 flux from the marshland occurred in the 1970s (Fig. 5b), together with the lowest precipitation (Fig. 6). After the 1970s, due to the higher air temperatures and precipitation in the 1980s and 1990s (Fig. 6), the area-weighted CH_4 flux reached its maximum value of $611.8 \pm 122.7\,\mathrm{kg\,ha^{-1}\,yr^{-1}}$ in the 1990s (Fig. 5b). Although the annual mean temperature was still high (3.93 °C) (Fig. 6), the mean annual area-weighted CH_4 flux was reduced to $505.6 \pm 109.8\,\mathrm{kg\,ha^{-1}\,yr^{-1}}$ (Fig. 5b) due to the lower precipitation in the 2000s (Fig. 6). Under the conditions of marshland being converted to cropland and climate change, the mean annual regional CH_4 emissions decreased by $1.3\,\mathrm{Tg\,yr^{-1}}$ in the 2000s compared with the average in the 1950s, with a 55 % reduction of the simulated average CH_4 emissions in the 1950s from the marshland (Fig. 5c). The average reduction rate was ~ 0.26 Tg per decade over the past 6 decades.

After marshland conversed to rice paddies, the CH_4 fluxes reduced remarkably (Fig. 5b). This corresponds to the measurements which indicated that marshland conversion to rice fields decreased CH_4 fluxes significantly, with a reduction of 28–73 % on the Sanjiang Plain (Huang et al., 2010). In rice fields, the mean annual area-weighted CH_4 flux has increased by ~ 150 % over the past 6 decades (Fig. 5b). The two most important reasons for this increase were that the grain yield in the 2000s was approximately 2 times higher than that in the 1950s, and the observed air temperature has increased significantly over the last 50 yr (Editorial Committee of China's National Assessment Report on Climate Change, 2007). A significant increase in the mean annual regional CH_4 emissions from rice fields has been observed since the 1980s (Fig. 5c), which corresponds to the increase in the area of rice fields (Fig. 5a).

As a result, the mean annual regional CH_4 emissions from the Sanjiang Plain decreased by $1.1\,\mathrm{Tg\,yr^{-1}}$ during the past 6 decades, ~ 46 % of the levels in the 1950s (Fig. 5b). The cumulative reduction in regional CH_4 emissions totaled 36 Tg over the past 5 decades relative to the average emissions in the 1950s (Fig. 5d). The cumulative reduction of CH_4 by ∼ 25 Tg resulting from the conversion of marshland to cropland and climate change over the 1960s-1990s (Fig. 5d) is comparable with the previous estimate of 27 Tg (Huang et al., 2010).

When simulating CH_4 emissions from marshland, there are also uncertainties due to certain assumptions about or simple spatialization of the model inputs. First, we used the available meteorological data from seven counties. For other counties or administrative farms, we used data from a neighboring site. This coarse spatial replacement may conceal the detailed spatial variation of climatic parameters to some extent. However, the differences in climate between the sites that cover the Sanjiang Plain are not significant. The standard deviations for precipitation and the air temperature are 33 mm (∼ 6 % of the average annual mean precipitation from 1950–2009 at the 7 sites) and 0.35 °C (∼ 10 % of the average annual mean air temperature from 1950–2009 at the 7 sites), respectively. Therefore, there may be little uncertainty caused by this coarse spatial replacement. Second, only the predominant plant species (*D. angustifolia* and *Carex* plants) were considered in this study. The average values obtained through measurements performed from 2002–2005 for *C. lasiocarpa* and from 2002–2004 for *D. angustifolia* were used as input data for the maximum above-ground biomass. However, large variation in maximum above-ground biomass values has been observed between different plant species, sites and years (Hao, 2006; Yang et al., 2002; Zhang et al., 2007). Variations of ±10 % in the maximum above-ground biomass would result in ∼ 10 % variation in the CH_4 flux (Table 2). Finally, the soil types are complex in the study area (Zhao, 1999). The soil input parameters we used may only represent the majority of soil types (meadow for *D. angustifolia*; humus for *C. lasiocarpa*). However, this assumption may induce little uncertainty because CH_4 emissions are not sensitive to the soil parameters (Table 2).

3.2.3 Spatial variation of CH_4 emissions

Using $CH4MOD_{wetland}$ and CH4MOD, the variations in the mean annual CH_4 emissions by county and administrative farm from marshland and rice paddies over the past 6 decades were simulated (Table E1 in Supplement E). Variations in the total amount of CH_4 emissions mainly occurred on the administrative farms (Table E1 in Supplement E), where extensive marshland conversion took place (Table D1 in Supplement D). For marshland, the mean annual amounts of CH_4 emissions decreased by 707.8×10^3 t and 613.1×10^3 t on the 3 administrative farms and in the 23 counties during the past 6 decades, accounting for 54 % and 46 % of the total reduction, respectively. For the rice paddies, the mean annual amounts of CH_4 emissions increased by 112.5×10^3 t and 75.3×10^3 t on the 3 administrative farms and in the 23 counties from the 1950s to the 2000s, accounting for 58 % and 42 % of the total increase, respectively (Table E1 in Supplement E). More specific details about the spatial variation of CH_4 emissions are given in Supplement E.

3.3 Impacts of marshland conversion and climate change on CH_4 emissions from marshland from 1950–2009

3.3.1 Changes in climatic factors from 1950–2009

Figure 6 shows the inter-annual and inter-decadal variations in the area-weighted air temperature (Fig. 6a), precipitation (Fig. 6b) and net radiation (Fig. 6c) on the Sanjiang Plain from 1950 to 2009. There is a significant increasing trend in the mean annual air temperature (linear trend with $P < 0.001$), with a rate of increase of 0.3 °C per decade being detected. An obvious increase in the air temperature has occurred since the 1980s, and the maximum mean annual temperature occurred in the 1990s (Fig. 6a). The mean annual precipitation and net radiation show great inter-annual variation, but without an obvious trend (linear trend with $P > 0.05$) (Fig. 6b, c). The minimum mean annual precipitation was observed in the 1970s, followed by the 2000s (Fig. 6b). The net radiation was low in the 1980s and 1990s (Fig. 6c).

These climatic factors can influence CH_4 emissions in three ways. First, a higher temperature will enhance the rate of microbial CH_4 production, and it will affect the length of the growing season by influencing the growing degree days (GDD). Second, increased precipitation may result in a higher water table position and subsequently increase CH_4 emissions. Third, higher net radiation could increase evapotranspiration and thereby lower the water table, which would decrease CH_4 emissions.

3.3.2 Impacts of marshland conversion and climate change on regional CH_4 emissions

Both marshland conversion and climate change have contributed to regional CH_4 decreases over the past 6 decades in the marshland of the Sanjiang Plain. If no climate change had taken place, marshland conversion alone could account for a cumulative CH_4 reduction of 33.6 Tg from 1960 to 2009 relative to the 1950s (calculated based on the simulated annual regional CH_4 emissions under scenario $S_{T,P,Rn}$). Climate change alone could account for a cumulative CH_4 reduction of 5.4 Tg from 1960 to 2009 relative to the 1950s (calculated based on the difference between the simulated annual regional CH_4 emissions under $A_{T,P,Rn}$ and scenario $S_{T,P,Rn}$). Figure 5 shows that the simulated cumulative CH_4 reduction under the conditions of climate change and marshland conversion was 39.0 Tg in the marshland (Fig. 5d). Thus, marshland conversion contributes 86 % of the regional reduction in CH_4 emissions, and climate change contributes 14 % from the marshland.

3.3.3 Impacts of climatic factors on regional CH_4 emissions

The impacts of climatic factors on the variation in regional CH_4 emissions are shown in Table 3. As the air temperature increases (Fig. 6a), the impact of the air temperature on regional CH_4 emissions shows a linear increase of 0.44 Tg per decade ($R = 0.83$, $P = 0.08$). The increasing air temperature enhanced regional CH_4 emissions significantly in the 1990s and 2000s (Table 3), corresponding to the obvious increase in air temperature in the 1990s and 2000s (Fig. 6a). The impacts of precipitation and net radiation on regional CH_4 emissions show obvious inter-decadal variation. Precipitation is the main contributor to regional CH_4 variation because it controls the water table position, which can markedly affect CH_4 fluxes (Fig. 2) (Boon et al., 1997; Ding et al., 2002). The maximum reduction in CH_4 emissions amounted to 4.09 Tg in the 1970s, followed by 2.80 Tg in the 2000s (Table 3), due to the lower precipitation in 1970s and 2000s (Fig. 6b). The influence of the inter-annual/inter-decadal variation in precipitation on regional CH_4 emissions may obscure the acceleration of CH_4 emissions caused by the increasing air temperature. Therefore, the concurrent influence of air temperature and precipitation ($IT_{T,P}$) shows a similar trend to the influence of precipitation alone (IT_P) on regional CH_4 emissions (Table 3).

3.3.4 Impacts of climatic factors on area-weighted CH_4 flux

The decadal and annual impacts of climatic factors on the area-weighted CH_4 flux in the marshland of the Sanjiang Plain are described in Table 3 and Fig. 7, respectively. A linear increase of 1.3 $kg\,ha^{-1}\,yr^{-1}$ was found with respect to the impact of the air temperature on the CH_4 flux over the past 6 decades (Fig. 7a). The negative impacts on the CH_4 flux have become lower, whereas significant positive impacts on the CH_4 flux have occurred since the 1990s (Table 3). Relative to the mean of the 1950s, the warming-induced increase in the area-weighted CH_4 flux averaged 19 $kg\,ha^{-1}\,yr^{-1}$ over the last two decades.

The annual impact of precipitation on the area-weighted CH_4 flux shows obvious inter-annual variation (Fig. 7b). It contributes a reduction of $\sim 1.5\,kg\,ha^{-1}\,yr^{-1}$ to the area-weighted CH_4 flux, although this is not statistically significant ($P > 0.2$) (Fig. 7b). This reduction is almost equal to the increase in the area-weighted CH_4 flux due to the air temperature (Fig. 7a). Lower precipitation in the 1970s (462 mm) and 2000s (486 mm) (Fig. 6b) caused the mean annual area-weighted CH_4 flux to decrease by $\sim 20\,\%$ relative to the 1950s (Table 3). Among the investigated climatic factors, precipitation is the main contributor to the reduction of the area-weighted CH_4 flux. We estimated that the relatively lower amount of precipitation over the period of 1960–2009 (averaging 47 $mm\,yr^{-1}$ lower than in the 1950s) contributed $\sim 91\,\%$ of the reduction in the area-weighted CH_4 flux among the climatic factors. This contribution of 91 %

was calculated using the equation $\frac{\overline{\mathrm{IF}_P^{1950\text{–}2009}}}{\overline{\mathrm{IF}_P^{1950\text{–}2009}}+\overline{\mathrm{IF}_T^{1950\text{–}2009}}}$, where $\overline{\mathrm{IF}_P^{1950\text{–}2009}}$ and $\overline{\mathrm{IF}_T^{1950\text{–}2009}}$ ($\mathrm{kg\,ha^{-1}\,yr^{-1}}$) (Eq. 5) represent the average impact of precipitation and air temperature on the area-weighted CH_4 flux from 1950–2009.

According to this analysis, although the air temperature increased continuously from the 1950s to the 1980s, it did not enhance the area-weighted CH_4 flux (Table 3). The reason for this lack of an effect is that the air temperature mainly increased during the growing season (April to October), rather than in winter (November to March), which reduces the number of days from germination to the occurrence of maximum above-ground biomass. An obvious rising trend was detected in the mean temperature of the growing season, which increased at a rate of 2.2 °C per decade (linear trend with $P < 0.05$) from 1950 to 1979, whereas no trend was found in winter temperatures (linear trend with $P > 0.2$) during the same period. In Northeast China, the required values of GDD are 50 °C· d and 2000 °C· d for plant germination and for approaching the maximum value, respectively (Li et al., 2010). The variation in temperature resulted in a decrease in the length of the days from germination to the occurrence of maximum above-ground biomass at a rate of 2.1 days per decade (linear trend with $P < 0.05$). According to the logistic equation that was used to calculate the daily above-ground biomass in $\mathrm{CH4MOD_{wetland}}$, the above-ground biomass will become infinitely close to the input maximum value as GDD reaches 2000 °C· d. The greater the number of days between germination and the occurrence of the maximum value, the closer the actual maximum above-ground biomass becomes to the input value. Therefore, the decrease in the number of days from germination to the maximum value resulted in a reduction of the actual maximum above-ground biomass value and, furthermore, decreased the maximum CH_4 flux value.

However, the positive impact of the air temperature on the area-weighted CH_4 flux during the last 60 yr may have been underestimated to some extent in this study. Due to the lack of biomass data in the study area for the last 60 yr, we simply assumed that the input maximum above-ground biomass was a constant value from 1950 to

2009. However, increasing air temperature may promote plant growth, increasing the maximum above-ground biomass over a long period. Therefore, the positive effect of climate warming on the CH_4 flux may have been underestimated to some extent. Additionally, the snowmelt process was not considered in the empirical water table model, and the resulting size and melt dates of the snow pack under higher winter temperatures may lead to earlier and larger rises in the water table, which, coupled with higher spring temperatures, could lengthen the duration of substantial CH_4 emissions as well as increase CH_4 emissions.

3.4 Projected impact of climate change on CH_4 fluxes by 2100

3.4.1 Projected climate change in the RCP scenarios

The climate projected by FGOALS shows a trend of becoming warmer and wetter in the RCP scenarios. The annual mean precipitation will increase in the range of 9 % to 12 % (46 and 63 mm) in the 2030s, 7 % to 17 % (38 and 90 mm) in the 2050s, and 12 % to 24 % (62 and 122 mm) in the 2080s relative to 1961–1990 (Table 4). No significant trend in precipitation was observed within the period from 2010–2100 in the RCP scenarios (Fig. F1 in Supplement F).

The annual mean area-weighted air temperature will increase by 49 % (1.5 °C yr^{-1}), 96 % (2.9 °C yr^{-1}), 150 % (4.6 °C yr^{-1}) and 238 % (7.3 °C yr^{-1}) by the 2080s relative to 1961–1990 in RCP 2.6, RCP 4.5, RCP 6.0 and RCP 8.5, respectively (Table 4). In RCP 2.6 scenario, the so-called “peak” scenario, the mean annual area-weighted air temperature will increase rapidly up to mid-century and then begin to decline (Fig. F1 in Supplement F), corresponding to the trend of radiative forcing (Moss et al., 2008). Under the “high pathway” (RCP 8.5) scenario, the projected change in the air temperature from 2010–2100 relative to 1961–1990 shows an obvious linear increase of 0.7 °C per decade ($P < 0.001$) (Fig. F1 in Supplement F). There is also an increasing trend in the projected change in the air temperature in the RCP 6.0 scenario, with a rate of 0.2 °C per decade ($P < 0.001$) (Fig. F1 in Supplement F).

3.4.2 Projected impact of climate change on CH4 fluxes by 2100

The projected area-weighted CH_4 fluxes are expected to be increased in the future due to rising air temperatures and precipitation (Table 4). In the "near term" of the 2030s (Moss et al., 2008), the differences regarding the increases of CH_4 fluxes are inconspicuous between the four RCP scenarios (Table 4). However, in the "long term" of the 2080s (Moss et al., 2008), the increase in the CH_4 flux is obviously higher under RCP 8.5 than the other RCP scenarios (Table 4). As the "high pathway" scenario, the RCP 8.5 scenario predicts that the area-weighted CH_4 fluxes will increase by 36 % in the 2030s, 80 % in the 2050s and 95 % in the 2080s compared with 1961–1990 (Table 4). In the RCP 6.0 scenario, the area-weighted CH_4 flux will increase by 50 % in the 2030s and 2050s and by 78 % in the 2080s (Table 4). Under the RCP 4.5 scenario, the increase of the area-weighted CH_4 flux is stabilized during the 21st century (Table 4 and Fig. F2 in Supplement F). The increase in the area-weighted CH_4 flux first reaches 46 % in the 2030s and then declines in the 2050s and 2080s in the RCP 2.6 scenario (Table 4).

The projected area-weighted CH_4 fluxes under the four RCP scenarios show obvious inter-annual variation (Fig. F2 in Supplement F) due to the yearly fluctuation of precipitation (Fig. F1 in Supplement F). Linear trend in the increase of CH_4 fluxes from 2010–2100 relative to 1961–1990 are shown in the RCP 6.0 and RCP 8.5 scenarios with rates of 23 $\mathrm{kg\,ha^{-1}\,yr^{-1}}$ and 48 $\mathrm{kg\,ha^{-1}\,yr^{-1}}$, respectively (Fig. F2 in Supplement F), which may be attributed to the air temperature (Fig. F1 in Supplement F).

Using a simulation modeling approach, Zhuang et al. (2006) projected that CH_4 emissions from the wetlands in northern high latitudes would more than double over the century under a scenario of projected atmospheric CO_2 mole fraction of approximately 1152 ppm by 2100. In the present study, the projected CH_4 flux would be ~ 2.1 times over the century, from 505 $\mathrm{kg\,ha^{-1}\,yr^{-1}}$ in the 2000s to 1060 $\mathrm{kg\,ha^{-1}\,yr^{-1}}$ in 2100, under the RCP 8.5 scenario of projected CO_2 concentrations of 1370 ppm. This increase is close to the increment reported by Zhuang et al. (2006). Under the doubled

CO_2 scenario (~ 700 ppm), increases of 56 % (Christensen and Cox, 1995) and 110 % (Shindell et al., 2004) have been estimated for the CH_4 flux in the northern high latitude region. The doubled CO_2 scenario is similar to the range between the RCP 6.0 scenario and RCP 8.5 scenario (650–850 ppm, Supplement C). Our results show increases of 56 % (from 505 kg ha^{-1} yr^{-1} in the 2000s to 790 kg ha^{-1} yr^{-1} in 2100) and 84 % (from 505 kg ha^{-1} yr^{-1} in the 2000s to 930 kg ha^{-1} yr^{-1} in 2100) under the RCP 4.5 scenario and RCP 6.0 scenario, respectively. These results are close to that of Christensen and Cox (1995), but lower than the estimate of Shindell et al. (2004). Thus, there is qualitative agreement among the existing studies that climate change can greatly enhance methane emissions from wetlands in the future, but the magnitude is uncertain. If the model considers the promoting effects of climate warming on snowmelt and plant growth, the projected CH_4 fluxes in the 21st century will be higher than the estimates presented here.

4 Conclusions

An estimated cumulative reduction of ~ 36 Tg in regional CH_4 emissions from the Sanjiang Plain of Northeast China occurred from 1960 to 2009 relative to the 1950s. Approximately 86 % of the reduction was attributed to extensive conversion of marshland to cropland over a total area of 3.2 M ha. Relatively low precipitation also contributed to the reduction in CH_4 emissions, while an increase in temperature obviously enhanced CH_4 emissions over the last two decades. Under the RCP scenarios, it is predicted that climate change will greatly enhance methane emissions from marshland on the Sanjiang Plain in the future.

Supplementary material related to this article is available online at: http://www.biogeosciences-discuss.net/9/5887/2012/bgd-9-5887-2012-supplement.pdf.

Acknowledgements. This work was supported by the National Natural Science Foundation of China (Grant No. 31000234, 41075107 and 41021004) and the Chinese Academy of Sciences (CAS) strategic pilot technology special funds (Grant No. XDA05020204). We are grateful to the members at the Sanjiang Wetland Experimental Station, Chinese Academy of Sciences for their contribution to the measurements of CH_4 emission, water table position and the plant biomass. We would also like to thank the National Meteorological Information Center of the China Meteorological Administration and the State Key Laboratory of Numerical Modeling for Atmospheric Sciences and Geophysical Fluid Dynamics of the Institute of Atmospheric Physics, Chinese Academy of Sciences for providing data.

References

Allen, R. G., Pereira, L. S., Raes, D., and Smith, M.: Crop evapotranspiration: guidelines for computing crop water requirements, in: Irrigation and Drainage Paper No. 56, FAO, Rome, Italy, available at: http://www.fao.org/docrep/X0490E/X0490E00.htm, 1998.

An, S. Q., Li, H. B., Guan, B. H., Zhou, C. F., Wang, Z. S., Deng, Z. F., Zhi, Y. B., Liu, Y. L., Xu, C., Fang, S. B., Jiang, J. H., and Li, H. L.: China's natural wetlands: past problems, current status, and future challenges, Ambio, 36, 335–342, 2007.

Beldring, S., Engen-Skaugen, T., Førland, E. J., and Roald, L. A.: Climate change impacts on hydrological processes in Norway based on two methods for transferring regional climate model results to meteorological station sites, Tellus A, 60, 439–450, 2008.

Bernie D.: Temperature implications from the IPCC 5th assessment Representative Concentration Pathways (RCP), Work stream 2, Report 11 of the AVOID programme (AV/WS2/D1/R11), available at: http://www.avoid.uk.net, 2010.

Bridgham, A. D., Megonigal, J. P., Keller, J. K., Bliss, N. B., and Trettin, C.: The carbon balance of North American wetlands, Wetlands, 26, 889–916, 2006.

Boon, P. I., Mitchell, A., and Lee, K.: Effects of wetting and drying on methane emissions from ephemeral floodplain wetlands in southeastern Australia, Hydrobiologia, 357, 73–87, 1997.

Cao, M. K., Gregson, K., and Marshall, S.: Global methane emission from wetlands and its sensitivity to climate change, Atmos. Environ., 32, 3293–3299, 1998.

Charmann, D. J. and Hendon, D.: Long-term changes in soil water tables over the past 4500 years: relationships with climate and North Atlantic atmospheric circulation and sea surface temperature, Climatic Change, 47, 45–59, 2000.

Christensen, T. R. and Cox, P.: Response of methane emission from arctic tundra to climate change: results from a model simulation, Geophys. Res. Lett., 31, L04501, doi:10.1029/2003GL018680, 1995.

Cui, B. S.: CH_4 emission from wetland in Sanjiang Plain, Sci. Geogr. Sin., 17, 93–95, 1997 (in Chinese with English abstract).

Ding, W. X. and Cai, Z. C.: Methane emission from natural wetlands in China: summary of years 1995–2004 studies, Pedosphere, 17, 475–486, 2007.

Ding, W. X., Cai, Z. C., Tsuruta, H., and Li, X. P.: 2002. Effect of standing water depth on methane emissions from freshwater marshes in Northeast China, Atmos. Environ., 36, 5149–5157, 2002.

Ding, W. X., Cai, Z. C., and Wang, D. X.: Preliminary budget of methane emissions from natural wetlands in China, Atmos. Environ., 38, 751–759, 2004.

Editorial Committee of China's National Assessment Report on Climate Change (Eds.): China's National Assessment Report on Climate Change, Science Press, Beijing, China, 2007 (in Chinese).

Gong, P., Niu, Z. G., Cheng, X., Zhao, K. Y., Zhou, D. M., Guo, J. G., Liang, L., Wang, X. F., Li, D. D., Huang, H. B., Wang, Y., Wang, K., Li, W. N., Wang, X. W., Ying, Q., Yang, Z. Z., Ye, Y. F., Li, Z., Zhuang, D. F., Chi, Y. B., Zhou, H. Z., and Yan, J.: China's wetland change (1990–2000) determined by remote sensing, Sci. China Earth Sci., doi:10.1007/s11430–010-4002-3, 2010.

Gedney, N., Cox, P. M., and Huntingford, C.: Climate feedback from wetland methane emissions, Geophys. Res. Lett., 31, L20503, doi:10.1029/2004GL020919, 2004.

Group of Chinese Wetland Resources Development and Environmental Protection: Development history of the Sanjiang Plain, Territ. Nat. Resour. Stud., 1, 15–19, 1998 (in Chinese).

Hao Q. J.: Effect of land-use change on greenhouse gases emissions in freshwater marshes in the Sanjiang Plain Ph.D. thesis, Institute of Atmospheric Physics, Chinese Academy of Sciences, Beijing, 205 pp., 2006 (in Chinese with English abstract).

Hay, L. E., Wilby, R. T., and Leavesley, G. H.: A comparison of delta change and downscaled GCM scenarios for three mountainous basins in the United States, J. Am. Water Resour. As., 36, 387–397, 2000.

Hulme, M., Conway, D., Jones, P. D., Jiang, T., Barrow, E. M., and Turney, C.: Construction of a 1961–1990 European climatology for climate change modelling and impact applications, Int. J. Climatol., 15 1333–1363, 1995.

Heilongjiang Provencal Bureau of Statistics (Eds.): Heilongjiang Provencal Bureau of Statistics, 2010, China Statistical Press, Beijing, China, 2010 (in Chinese).

Huang, Y., Zhang, W., Zheng, X. H., Li, J., and Yu, Y. Q.: Modeling methane emission from rice paddies with various agricultural practices, J. Geophys. Res., 109, D08113, doi:10.1029/2003JD004401, 2004.

Huang, Y., Zhang, W., Zheng, X. H., Han, S. H., and Yu, Y. Q.: Estimates of methane emissions from Chinese rice paddies by linking a model to GIS database, Acta Ecological Sinca, 26, 980–988, 2006.

Huang, Y., Sun, W., Zhang, W., Yu, Y., Su, Y., and Song, C.: Marshland conversion to cropland in Northeast China from 1950 to 2000 reduced the greenhouse effect, Global Change Biol., 16, 680–695, 2010.

IPCC: Climate Change 2007: The Physical Science Basis, Summary for Policymakers, Contribution of Working Group I to the Fourth Assessment Report of the Intergovernmental Panel on Climate Change, Intergovernmental Panel on Climate Change, Paris, France, 2007.

Jia, Z. J., Zhang, W., Huang, Y., Song, C. C., and Zhao, X. S.: Effects of marshland reclamation on evapotranspiration in the Sanjiang Plain, Environ. Sci., 31, 833–842, 2010 (in Chinese with English abstract).

Li, C. S., Cui, J. B., Sun, G., and Trettin, C.: Modeling impacts of management on carbon sequestration and trace gas emissions in forested wetland ecosystems, Environ. Manage., 33, 176–186, 2004.

Li, T. T., Huang, Y., Zhang, W., and Song, C. C.: CH4MOD$_{\text{wetland}}$: A biogeophysical model for simulating CH_4 emissions from natural wetland, Ecol. Model., 221, 666–680, 2010.

Liu, X. T. and Ma, X. H.: Influence of large scale reclamation on natural environment and regional environmental protection in the Sanjiang Plain, Sci. Geogr. Sin., 20, 14–19, 2000 (in Chinese with English abstract).

Ma, Z.: Protection, development and economic evaluation of the Sanjiang Plain, Ph.D. thesis, Renmin University of China, Beijing, 1999 (in Chinese with English abstract).

Mitsch, J. W. and Gosselink, J. G.: Wetlands, 4th edn, John Wiley and Sons Inc, Hoboken, NJ, 2007.

Moss, R., Babiker, M., Brinkman, S., Calvo, E., Carter, T., Edmonds, J., Elgizouli, I., Emori, S., Erda, L., Hibbard, K., Jones, R., Kainuma, M., Kelleher, J., Lamarque, J. F., Manning, M., Matthews, B., Meehl, J., Meyer, L., Mitchell, J., Nakicenovic, N., O'Neill, B., Pichs, R., Riahi, K., Rose, S., Runci, P., Stouffer, R., van Vuuren, D., Weyant, J., Wilbanks, T., van Ypersele, J. P., and Zurek, M.: Towards new scenarios for analysis of emissions, climate change, impacts, and response strategies, Technical summary Intergovernmental Panel on Climate Change, Geneva, 25 pp., 2008.

Ning, J., Zhang, S. W., Li, Y., and Wang, L.: Analysis on wetland shrinking characteristics and its cause in Heilongjiang province for the last 50 years, J. Nat. Resour., 23, 79–86, 2008 (in Chinese with English abstract).

Priestley, C. H. B. and Taylor, R. J.: On the assessment of surface heat flux and evaporation using large-scale parameters, Mon. Weather Rev., 100, 81–92, 1972.

Prudhomme, C., Reynard, N., and Crooks, S.: Downscaling of global climate models for flood frequency analysis: where are we now? Hydrol. Process., 16, 1137–1150, 2002.

Ramsar Convention Secretariat (Eds.): Ramsar Handbook for the Wise Use of Wetlands, 2nd Edition Handbook 10, Wetland Inventory: A Ramsar Framework for Wetland Inventory Ramsar secretariat, Gland, Switzerland, 2004.

Revenga, C., Brunner, J., Henninger, N., Kassem, K., and Payne, R. (Eds.): Pilot Analysis of Global Ecosystems, Freshwater Systems World Resources Institute, Washington, DC, 65 pp., 2000.

Shindell, D. T., Walter, B. P., and Faluvegi, G.: Impacts of climate change on methane emissions from wetlands, Geophys. Res. Lett., 31, L21202, doi:10.1029/2004GL021009, 2004.

Shuttleworth, W. J.: Evaporation, in: Handbook of Hydrology, edited by: Maidment, D. R., McGraw-Hill, New York, USA, 4.1–4.53, 1992.

Song, C. C., Zhang, J. B., Wang, Y. Y., Wang, Y. S., and Zhao, Z. C.: Emission of CO_2, CH_4 and N_2O from freshwater marsh in northeast of China, J. Environ. Manage., 40, 6879–6885, 2007.

Song, C. C., Xu, X. F., Tian, H. Q., and Wang, Y. Y.: Ecosystematmosphere exchange of CH_4 and N_2O and ecosystem respiration in wetlands in the Sanjiang Plain, Northeastern China, Global Change Biol., 15, 692–705, 2009.

Strack, M., Waddington, M., Turetsky, M., Roulet, N. T., and Byrne, K. A.: Northern peatlands, greenhouse gas exchange and climate change, in: Peatlands and Climate Change, Chapter 2, edited by: Strack, M., International Peat Society, Vapaudenkatu Jyväskylä, Finland, 44–69, 2008.

Su, Y. H. and Zhang, W.: Building up annual series of cropland acreage in Sanjiang Plain in the last 50 years, Geography and Geo-Information Science, 24, 72–75, 2008 (in Chinese with English abstract).

Sun, L. and Song, C. C.: Evapotranspiration from a freshwater marsh in the Sanjiang Plain, Northeast China, J. Hydrol., 352, 202–210, 2008.

Thomas, C., Miao, S., and Sindhøj, E.: Environmental factors affecting temporal and spatial patterns of soil redox potential in Florida Everglades wetlands, Wetlands, 29, 1133–1145, 2009.

Updegraff, K., Bridgham, S. D., Pastor, J., Weishampel, P., and Harth, C.: Response of CO_2 and CH_4 emissions from peatlands to warming and water table manipulation, Ecol. Appl., 11, 311–326, 2001.

Vepraskas, M. J. and Caldwell, P. V.: Interpreting morphological features in wetland soils with a hydrological model, Catena, 73, 153–165, 2008.

Wang, A. H., Zhang, S. Q., and He, Y. F.: Study on dynamic change of mire in Sanjiang Plain based on RS and GIS, Sci. Geogr. Sin., 22, 636–640, 2002 (in Chinese with English abstract)

Wang, A. H., Zhang, S. Q., and Zhang, B.: A study on the change of spatial pattern of wetland in the Sanjiang Plain, Acta Ecological Sinca, 23, 237–243, 2003 (in Chinese with English abstract).

Wang, Z. M., Zhang, B., Zhang, S. Q., Li, X. Y., Liu, D. W., Song, C. C., Li, J. P., Li, F., and Duan, H. T.: Changes of land use and of ecosystem service values in Sanjiang Plain, Northeast China, Environ. Monit. Assess., 112, 69–91, 2006.

Wang, Z. M., Song, K. S., Liu, D. W., Zhang, B., Zhang, S. Q., Li, F., Ren, C. Y., Jin, C., Yang, T., and Zhang, C. H.: Process of land conversion from marshland into cropland in the Sanjiang Plain during 1954–2009, Wetland Sci., 7, 208–217, 2009 (in Chinese with English abstract).

Wilby, R. L., Charles, S. P., Zorita, E., Timbal, B., Whetton, P., and Mearns, L. O.: Guidelines for use of climate scenarios developed from statistical downscaling methods, Supporting material of the Intergovernmental Panel on Climate Change, available from the DDC of IPCC TGCIA, 27, 2004.

Yang, Y., Wang, S., He, T., Tian, K., and Yang, B.: Study on plant biomass and its seasonal dynamics of typical wetland ecosystems in the Sanjiang Plain, Grassland China, 24, 1–7, 2002 (in Chinese with English abstract).

Yang, W. Y., Song, C. C., Zhang, J. B: Dynamics of methane emissions from a freshwater marsh of Northeast China, Sci. Total Environ., 371, 286–292, 2006.

Yu, Y., Yu, R., Zhang, X., and Liu H.: A flexible coupled ocean-atmosphere general circulation-mode1, Adv. Atmos. Sci., 19, 169–190, 2002.

Yu, Y., Zhang, X., and Guo, Y.: Global coupled ocean-atmosphere general circulation models in LASG/IAP, Adv. Atmos. Sci., 21, 444–455, 2004.

Zhang, Y., Li, C. S., Trettin, C. C., Li, H., and Sun, G.: An integrated model of soil, hydrology, and vegetation for carbon dynamics in wetland ecosystems, Glob. Biogeochem. Cy., 16, 1061, doi:10.1029/2001GB001838, 2002.

Zhang, S. Q., Wang, A. H., Zhang, J. Y., and Zhang, B.: The spatial temporal dynamic characteristics of the marsh in the Sanjiang Plain, J. Geogr. Sci., 13, 201–207, 2003.

Zhang, S. W., Zhang, Y. Z., L, Y., and Chang, L. P.: Spatial and temporal variations in marshlands and its ecological effects, in: Analysis of the Spatial and Temporal Characteristics of Landuse and Cover in the Northeast, Chapter 7, edited by: Zhang, S. W., Zhang, Y. Z., L, Y., and Chang, L. P., Science Press, Beijing, China, 279–312, 2006 (in Chinese).

Zhang, L. H., Song, C. C., Zheng, X. H., Wang, D. X., and Wang, Y. Y.: Effects of nitrogen on the ecosystem respiration, CH_4 and N_2O emissions to the atmosphere from the freshwater marshes in Northeast China, Environ. Geol., 52, 529–539, 2007.

Zhang, J., Ma K., and Fu, B.: Wetland loss under the impact of agricultural development in the Sanjiang Plain, NE China, Environ. Monit. Assess., 166, 139–148, 2010.

Zhao, C. Y., Ren, G. Y., Zhang, Y. F., and Wang, Y.: Climate change of the Northeast China over the past 50 years, J. Arid Land Resour. Environ., 23 , 25–30, 2009 (in Chinese with English abstract).

Zhao, K. Y. (Ed.): Wetlands in China, Science Press, Beijing, China, 181–245, 1999 (in Chinese).

Zhao, X. S., Huang, Y., Jia, Z. J., Liu, H. Z., Song, T., Wang, Y. S., Shi, L. Q., Song, C. C., and Wang, Y. Y.: Effects of the conversion of marshland to cropland on water and energy exchanges in Northeastern China, J. Hydrol., 355, 181–191, 2008.

Zhuang, Q. L., Mellillo, J. M., Sarofim, M. C., Kicklighter, D. W., McGuire, A. D., Felzer, B. S., Sokolov, A., Prinn, R. G., Steudle, P. A., and Hu, S. M.: CO_2 and CH_4 exchanges between land ecosystems and the atmosphere in northern high latitudes over the 21st century, Geophys. Res. Lett., 33, L17403, doi:10.1029/2006GL026972, 2006.

Table 1. Description of the climate conditions for simulating CH_4 emissions from 1950–2009.

Climate	Actual climate	Scenario			
	$A_{T,P,Rn}$	$S_{T,P,Rn}$	$S_{T,P}$	S_T	S_P
T_{air}	1950–2009	1950–1959	1950–1959	1950–1959	1950–2009
P	1950–2009	1950–1959	1950–1959	1950–2009	1950–1959
R_{n}	1950–2009	1950–1959	1950–2009	1950–2009	1950–2009

Title Page

Abstract | Introduction

Conclusions | References

Tables | Figures

◀◀ | ▶▶

◀ | ▶

Back | Close

Full Screen / Esc

Printer-friendly Version

Interactive Discussion

Table 2. Model sensitivity analysis.

Environmental drivers/ Model input	Baseline		Change	$\Delta CH_4/CH_{4\_baseline}$ (%)			
				2003		2004	
	DA[a]	CL[b]		DA[a]	CL[b]	DA[a]	CL[b]
T_{air} (°C)	–	–	+2/–2	+28.8/–23.9	+27.3/–19.2	+41.5/–31.5	+23.4/–19.7
WD (cm)	–	–	+5/–5	+269.9/–90.0	121.8/–57.7	398.2/–42.3	+13.2/–5.5
W_{max} (g m^{-2})	485	450	+10%/–10%	+10.0/–10.0	+10.9/–10.7	+8.3/–8.5	+10.1/–10.4
SAND	47	56	+10%/–10%	+0.2/–0.2	+0.4/–0.3	+0.2/–0.2	+0.3/–0.3
ρ (g cm^{-3})	1	0.74	+10%/–10%	+0.2/–0.2	+0.5/–0.4	+0.3/–0.3	+0.4/–0.4
SOM (g kg^{-1})	70	246	+10%/–10%	+0.2/–0.2	+0.5/–0.4	+0.3/–0.3	+0.4/–0.4

[a] DA represents *Deyeuxia angustifolia* site

[b] CL represents *Carex lasiocarpa* site

Table 3. Impact of climatic factors on CH_4 variation.

Decade	Impact on regional CH_4 emissions (Tg)[a]				Impact on area-weighted CH_4 flux[b]			
	IT_T	IT_P	$IT_{T,P}$	$IT_{T,P,Rn}$	P_T	P_P	$P_{T,P}$	$P_{T,P,Rn}$
1960s	−1.10	0.16	−0.56	−0.24	−5.7 %	1.7 %	−2.6 %	−1.0 %
1970s	−1.08	−4.09	−4.32	−4.10	−5.6 %	−21.1 %	−22.7 %	−21.6 %
1980s	−0.01	−1.78	−1.24	−0.75	−0.2 %	−9.4 %	−6.5 %	−3.9 %
1990s	0.82	0.11	0.96	1.57	5.1 %	0.4 %	7.2 %	10.8 %
2000s	0.13	−2.80	−2.15	−1.86	1.7 %	−21.1 %	−14.9 %	−12.2 %

[a] Used Eq. (4), positive/negative values represent increase/decrease regional CH_4 emissions.

[b] Used Eq. (5), positive/negative values represent increase/decrease area-weighted CH_4 flux.

IT_T: Impact of air temperature on regional CH_4 emissions
IT_P: Impact of precipitation on regional CH_4 emissions
$IT_{T,P}$: Impact of air temperature and precipitation on regional CH_4 emissions
$IT_{T,P,Rn}$: Impact of air temperature, precipitation and net radiation on regional CH_4 emissions
P_T: Impact of air temperature on area-weighted CH_4 flux
P_P: Impact of precipitation on area-weighted CH_4 flux
$P_{T,P}$: Impact of air temperature and precipitation on area-weighted CH_4 flux
$P_{T,P,Rn}$: Impact of air temperature, precipitation and net radiation on area-weighted CH_4 flux

Title Page
Abstract Introduction
Conclusions References
Tables Figures
|◀ ▶|
◀ ▶
Back Close
Full Screen / Esc
Printer-friendly Version
Interactive Discussion

Table 4. Projected increases in area-weighted CH_4 flux relative to 1961–1990.

Decade	RCP 2.6			RCP 4.5			RCP 6.0			RCP 8.5		
	P^a	T^b	$CH_4{}^c$	P^a	T^b	$CH_4{}^c$	P^a	T^b	$CH_4{}^c$	P^a	T^b	$CH_4{}^c$
2030S	10 %	83 %	46 %	11 %	86 %	45 %	12 %	113 %	50 %	9 %	96 %	36 %
2050S	7 %	70 %	27 %	14 %	124 %	57 %	10 %	127 %	50 %	17 %	170 %	80 %
2080S	12 %	49 %	36 %	16 %	96 %	52 %	24 %	150 %	78 %	17 %	238 %	95 %

[a] Increase in precipitation relative to the baseline of 1961–1990 (515 mm)

[b] Increase in temperature relative to the baseline of 1961–1990 (3.07 °C)

[c] Increase in the simulated area-weighted CH_4 flux relative to the baseline of 1961–1990 (513 kg ha^{-1} yr^{-1})

Fig. 1. The study area on the Sanjiang Plain of Northeast China, covering 23 counties and 3 administrative farms.

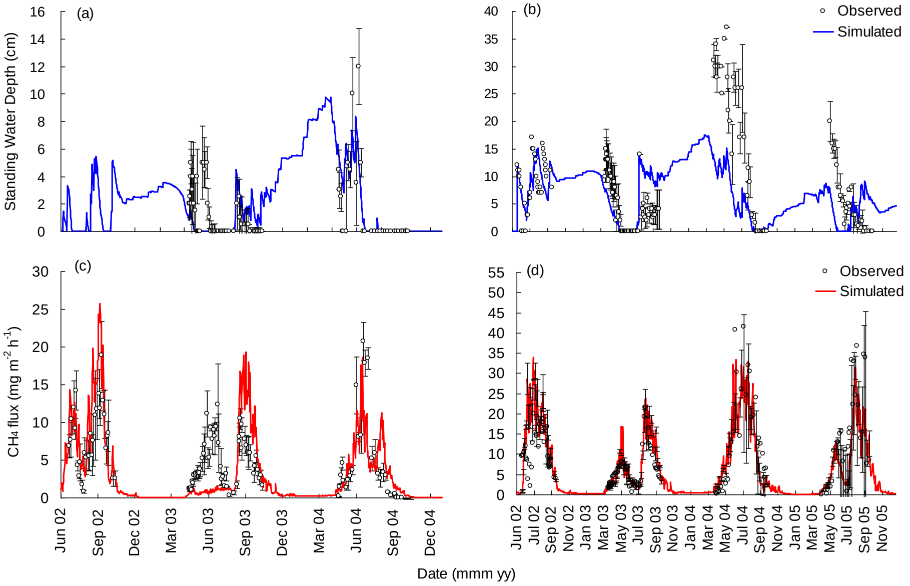

Fig. 2. Comparison of simulated and observed seasonal patterns of standing water depth and CH_4 fluxes on the Sanjiang Plain. **(a)** Standing water depth and **(c)** CH_4 flux for *Deyeuxia angustifolia* site; **(b)** Standing water depth and **(d)** CH_4 flux for *Carex lasiocarpa* site. The vertical bars are standard deviations from 3 sampling replicates.

Title Page
Abstract
Introduction
Conclusions
References
Tables
Figures
◀◀
▶▶
◀
▶
Back
Close
Full Screen / Esc
Printer-friendly Version
Interactive Discussion

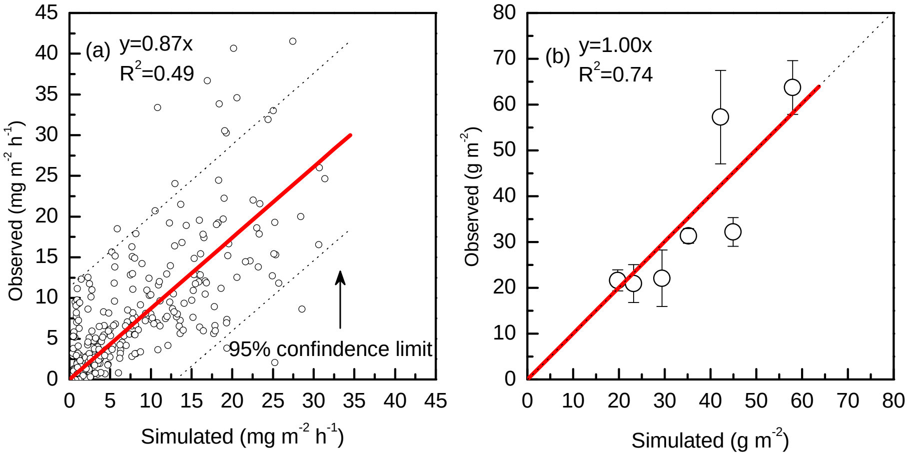

Fig. 3. Observed vs. simulated CH_4 emissions from *Deyeuxia angustifolia* site (June 2002–December 2004) and *Carex lasiocarpa* site (June 2002–December 2005) on the Sanjiang Plain. **(a)** CH4 fluxes, dashed lines are 95 % confidence limits. **(b)** Total amount of annual/seasonal CH_4 emissions, dashed line is 1 : 1, the vertical bars are standard deviations from 3 sampling replicates.

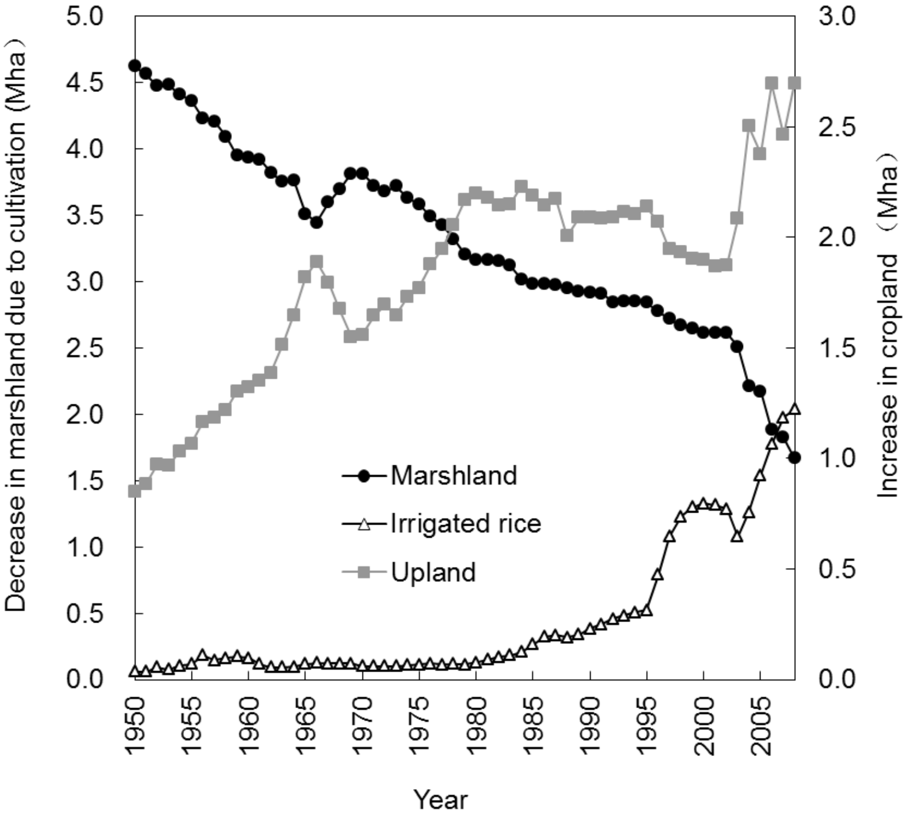

Fig. 4. Conversion of marshland to cropland on the Sanjiang Plain.

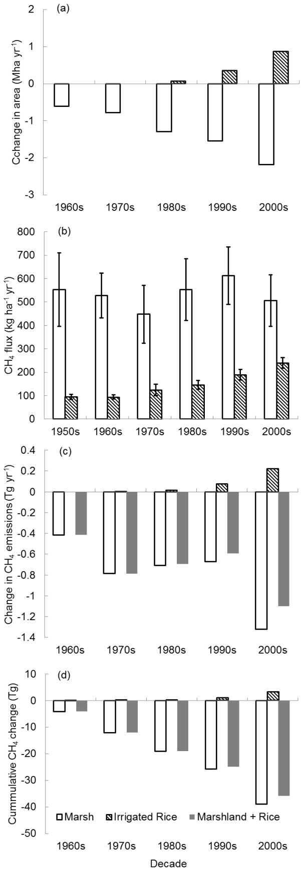

Fig. 5. Decadal variations in area and CH$_4$ emission. **(a)** Decadal variations in area relative to the average1950s. **(b)** Inter-decadal variations in the area-weighted CH$_4$ flux, the vertical bars are standard deviations of 10 yr of each decade. **(c)** Decadal variations in regional CH$_4$ emissions relative to the average 1950s. **(d)** Cumulative CH$_4$ change relative to the average 1950s.

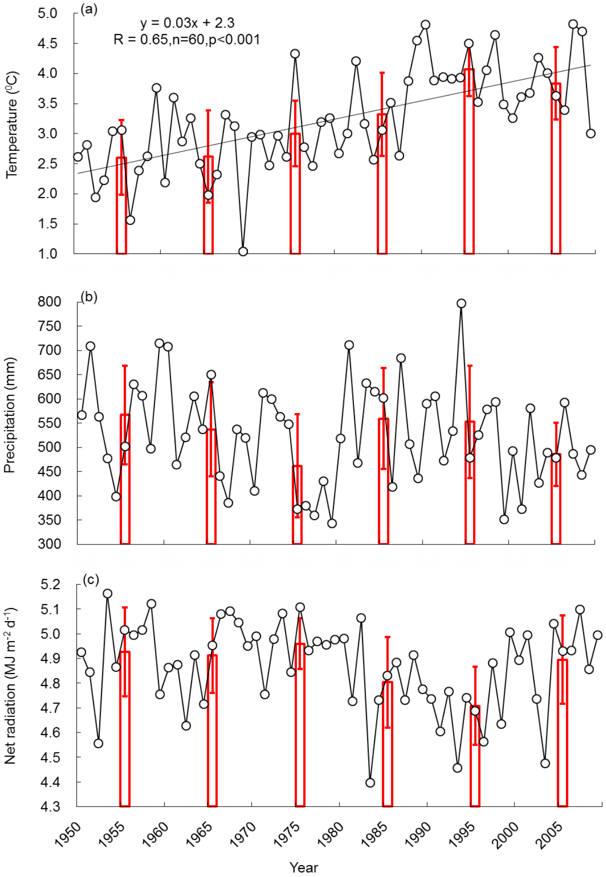

Fig. 6. Variations in the area-weighted air temperature **(a)**, precipitation **(b)** and net radiation **(c)** on the Sanjiang Plain from 1950 to 2009. Solid lines represent the inter-annual variations; Columns represent the inter-decadal variations, the vertical bars are standard deviations of 10 yr of each decade.

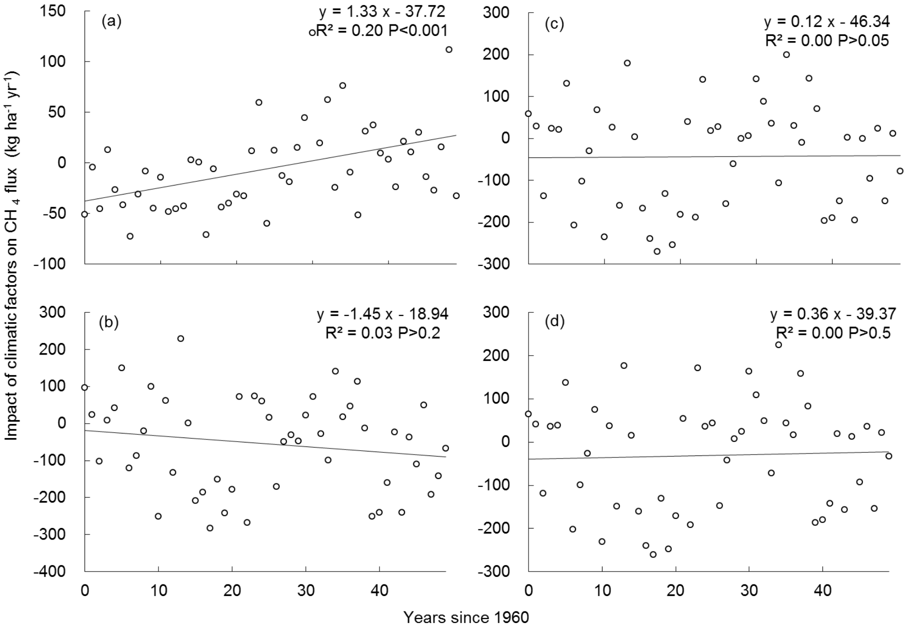

Fig. 7. Impact of air temperature **(a)**, precipitation **(b)**, air temperature and precipitation **(c)**, air temperature, precipitation and net radiation **(d)** on area-weighted CH_4 flux. Estimated IF^{i}_{CF} by Eq. (4).